Protein Engineering of Toluene 4-Monooxygenase of *Pseudomonas mendocina* KR1 for Synthesizing 4-Nitrocatechol From Nitrobenzene

Ayelet Fishman,[1] Ying Tao,[1] William E. Bentley,[2] Thomas K. Wood[1]

[1]Departments of Chemical Engineering and Molecular and Cell Biology, University of Connecticut, Storrs, Connecticut 06269-3222; telephone: 860-486-2483; fax: 860-486-2959; e-mail: twood@engr.uconn.edu
[2]Department of Chemical Engineering, University of Maryland, College Park, Maryland

Received 29 February 2004; accepted 11 May 2004

Published online 19 August 2004 in Wiley InterScience (www.interscience.wiley.com). DOI: 10.1002/bit.20185

Abstract: After discovering that toluene 4-monooxygenase (T4MO) of *Pseudomonas mendocina* KR1 oxidizes nitrobenzene to 4-nitrocatechol, albeit at a very low rate, this reaction was improved using directed evolution and saturation mutagenesis. Screening 550 colonies from a random mutagenesis library generated by error-prone PCR of *tmoAB* using *Escherichia coli* TG1/pBS(Kan)T4MO on agar plates containing nitrobenzene led to the discovery of nitrocatechol-producing mutants. One mutant, NB1, contained six amino acid substitutions (TmoA Y22N, I84Y, S95T, I100S, S400C; TmoB D79N). It was believed that position I100 of the α subunit of the hydroxylase (TmoA) is the most significant for the change in substrate reactivity due to previous results in our lab with a similar enzyme, toluene *ortho*-monooxygenase of *Burkholderia cepacia* G4. Saturation mutagenesis at this position resulted in the generation of two more nitrocatechol mutants, I100A and I100S; the rate of 4-nitrocatechol formation by I100A was more than 16 times higher than that of wild-type T4MO at 200 μM nitrobenzene (0.13 $\pm$ 0.01 vs. 0.008 $\pm$ 0.001 nmol/min·mg protein). HPLC and mass spectrometry analysis revealed that variants NB1, I100A, and I100S produce 4-nitrocatechol via *m*-nitrophenol, while the wild-type produces primarily *p*-nitrophenol and negligible amounts of nitrocatechol. Relative to wild-type T4MO, whole cells expressing variant I100A convert nitrobenzene into *m*-nitrophenol with a V_{max} of 0.61 $\pm$ 0.037 vs. 0.16 $\pm$ 0.071 nmol/min·mg protein and convert *m*-nitrophenol into nitrocatechol with a V_{max} of 3.93 $\pm$ 0.26 vs. 0.58 $\pm$ 0.033 nmol/min·mg protein. Hence, the regiospecificity of nitrobenzene oxidation was changed by the random mutagenesis, and this led to a significant increase in 4-nitrocatechol production. The regiospecificity of toluene oxidation was also altered, and all of the mutants produced 20% *m*-cresol and 80% *p*-cresol, while the wild-type produces 96% *p*-cresol. Interestingly, the rate of toluene oxidation (the natural substrate of the enzyme) by I100A was also higher by 65% (7.2 $\pm$ 1.2 vs. 4.4 $\pm$ 0.3 nmol/min·mg protein). Homology-based modeling of TmoA suggests reducing the size of the side chain of I100 leads to an increase in the width of the active site channel, which facilitates access of substrates and promotes more flexible orientations. © 2004 Wiley Periodicals, Inc.

Keywords: protein engineering; toluene 4-monooxygenase; *Pseudomonas mendocina* KR1; 4-nitrocatechol; nitrobenzene

INTRODUCTION

Biocatalysis has become an increasingly important technology for producing compounds of high-added value for the chemical industry (Huisman and Gray, 2002; Schmid et al., 2002). Since the year 2000, more than 400 patents on the use of microorganisms or enzymes to produce specialty chemicals have been issued (Rouhi, 2003). It is predicted, that by the year 2050, biocatalysis and biotransformations will account for 30% of the chemical business (van Beilen et al., 2003). Among the various classes of enzymes, oxygenases are considered one of the most promising due to their ability to perform selective hydroxylations that are not accessible by chemical methods (van Beilen et al., 2003). One recent commercial example is the production of an intermediate for an antilipolytic drug from the oxidation of 2,5-dimethylpyrazine to 5-methylpyrazine-2-carboxylic acid with whole cells of *Pseudomonas putida* ATCC 33015 expressing xylene monooxygenase (Schmid et al., 2001).

Nitrocatechols have been found to be useful intermediates for the synthesis of pharmaceuticals such as Flesinoxan, an antihypertensive drug (Hartog and Wouters, 1988; Scharrenburg and Frankena, 1996). Recently, nitrocatechol compounds were discovered as potent inhibitors of catechol-*o*-methyltransferase and are under clinical evaluation for the treatment of Parkinson's disease and other

Correspondence to: Thomas K. Wood
Contract grant sponsors: National Science Foundation; U.S. Environmental Protection Agency
Contract grant number: BES-0124401

nervous system disorders (Learmonth and Freitas, 2002; Learmonth et al., 2002). In another study, 4-nitrocatechol (4-NC) and 3-nitrocatechol (3-NC) were found to be competitive inhibitors of nitric oxide synthase with potential anti-nociceptive (pain-relieving) activity (Palumbo et al., 2002). As chemical synthesis of these compounds is problematic in terms of yield and selectivity (Palumbo et al., 2002), the utilization of oxygenases is advantageous. The high redox potential of oxygenases enables them to perform reactions with chemically stable substrates as well as provide a high degree of regio- and enantioselectivity (Burton, 2003; Li et al., 2002). Transforming selectively an inexpensive and abundant chemical as nitrobenzene (NB) into a valuable feedstock for drug production, namely 4-NC, is therefore of great significance.

There have been previous reports in the literature on oxygenases capable of producing nitrocatechols. *p*-Nitrophenol hydroxylase of *Arthrobacter sp*. and *Bacillus sphaericus* JS905 transforms *p*-nitrophenol (*p*-NP) to 4-NC often with further removal of the nitro group to obtain 1,2,4-trihydroxybenzene (Jain et al., 1994; Kadiyala and Spain, 1998). Kieboom and co-workers screened 21 microorganisms for their ability to convert nitroaromatics into 3-NC (Kieboom et al., 2001). Strains containing toluene-dioxygenases from *P. putida* F1, *Nocardia* S3, *Pseudomonas* JS150, *Cornybacterium* C125, and *Xanthobacter* 124X were able to transform NB to 3-NC rapidly. They did not report a toluene monooxygenase-containing strain able to perform this reaction. Haigler and Spain (1991) reported *Pseudomonas mendocina* KR1 and *Ralstonia pickettii* PKO1 convert NB to NC; however, the enzymes responsible for the addition of the second hydroxyl group to the nitrophenols to form nitrocatechols were not identified.

Toluene-4-monooxygenase (T4MO) is a soluble diiron monooxygenase belonging to the group of four component alkene/aromatic monooxygenases (Leahy et al., 2003). It is composed of six genes designated *tmoABCDEF*. The genes *tmoA*, *tmoB,* and *tmoE* encode the α, γ, and β subunits, respectively, of the hydroxylase component (212 kDa with $\alpha_2\beta_2\gamma_2$ quaternary structure), which was recently described as responsible for the regiospecificity of the enzyme (Mitchell et al., 2002; Pikus et al., 2000). The *tmoC* gene encodes a Rieske-type [2Fe-2S] ferredoxin (12.5 kDa), and *tmoD* encodes a catalytic effector protein (11.6 kDa). The binding of the effector protein has been shown to enhance the catalytic rate of the enzyme and to refine the product distribution leading to the high regiospecificity of T4MO (Mitchell et al., 2002). Gene *tmoF* encodes an NADH oxidoreductase (33 kDa). Due to the complex nature of monooxygenases, biological oxidation reactions are often performed using growing or resting cells (Li et al., 2002; Oppenheim et al., 2001; Schmid et al., 2001).

T4MO is a highly regiospecific enzyme, hydroxylating nearly all monosubstituted benzenes tested including toluene, chlorobenzene, methoxybenzene, and nitrobenzene at the *para* position (Mitchell et al., 2002). Recent mechanistic studies reveal that active site-directed opening of an epoxide intermediate may account for this high regiospecificity (Mitchell et al., 2003). T4MO has been shown to perform single hydroxylations, transforming benzene to phenol, toluene to *p*-cresol and other monosubstituted benzenes to the subsequent *p*-hydroxylated compounds (Pikus et al., 1997). Wood and co-workers have recently reported that T4MO expressed in *Escherichia coli* TG1 cells can perform successive hydroxylations, resulting in conversion of benzene to 1,2,3-trihydroxybenzene (Tao et al., 2004). Nevertheless, there is no evidence to date of T4MO being able to convert substituted benzenes (e.g., nitrobenzene) to their respective catechols (e.g., nitrocatechol).

Our work shows that wild-type T4MO can in fact hydroxylate NB sequentially to 4-NC albeit at a very slow rate. The goals of this study were to generate mutants of T4MO with high 4-NC formation rates and to elucidate the pathway by which they perform the double hydroxylation from NB. Both error-prone PCR and saturation mutagenesis were used to alter the substrate specificity of wild-type T4MO, and the apparent kinetic constants for wild-type T4MO and the variants were determined. The altered activity and specificity of the mutants was interpreted using three-dimensional homology modeling.

MATERIALS AND METHODS

Chemicals, Bacteria, and Growth Conditions

NB was purchased from Fisher Scientific Co. (Fairlawn, NJ) and 4-NC, *p*-cresol, *o*-, *m*-, and *p*-nitrophenol were obtained from Acros Organics (Morris Plains, NJ). *o*-Cresol and *m*-cresol were obtained from Aldrich Chemical Co. (Milwaukee, WI). All materials used were of the highest purity available and were used without further purification.

Escherichia coli strain TG1 (*supE hsd*Δ5 *thi* Δ (*lac-proAB*) F′[*traD*36 *proAB*$^+$ *lacI*^{q} *lacZ*ΔM15]) (Sambrook et al., 1989) was utilized as the host for gene cloning and expression. TG1 was routinely cultivated at 37°C in Luria-Bertani (LB) medium (Sambrook et al., 1989) with kanamycin (100 μg/mL) added to maintain the vector pBS(Kan)T4MO (Tao et al., 2004) which expresses the *tmoABCDEF* genes from a constitutive *lac* promoter and which avoids feeder colonies due to the kanamycin resistance marker (Fig. 1). Expression of wild-type T4MO from pBS(Kan)T4MO within *E. coli* strains produced blue-colored cells on agar plates and in broth cultures. The blue color is indicative of indigo, formed by oxidation of indole from tryptophan (Eaton and Chapman, 1995).

Protein Analysis and Plasmid Manipulation

The Total Protein Kit (Sigma Chemical Co.) was used to determine the total cellular protein of *E. coli* TG1/pBS(Kan)T4MO [henceforth TG1(T4MO)] for calculation

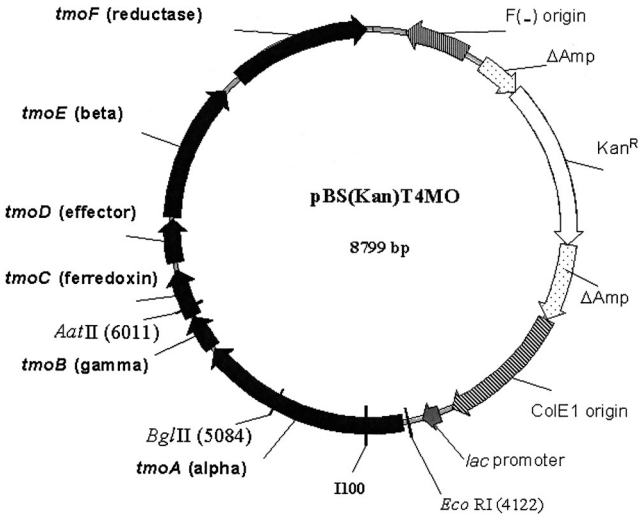

Figure 1. Vector pBS(Kan)T4MO for constitutive expression of wild-type T4MO and mutants. Kan^R is the kanamycin resistance gene. The six genes coding for T4MO are *tmoABE* (hydroxylase $A_2B_2E_2$), *tmoC* (ferredoxin), *tmoD* (effector protein), and *tmoF* (NADH-ferredoxin oxidoreductase).

of whole-cell specific activities. Cellular protein samples of cell grown with and without 1 m*M* isopropyl β-D-thiogalactopyranoside were analyzed on standard 12% Laemmli discontinuous sodium dodecyl sulfate (SDS)-polyacrylamide gels (Sambrook et al., 1989). Plasmid DNA was isolated using a Midi or Mini Kit (Qiagen, Inc., Chatsworth, CA), and DNA fragments were isolated from agarose gels using the GeneClean III Kit (Bio 101, Vista, CA). *Escherichia coli* strains were transformed by electroporation using a Bio-Rad GenePulser/Pulse Controller (Hercules, CA) at 15 kV/cm, 25 μF, and 200 Ω.

Random Mutagenesis

The *tmoAB* genes, α and γ hydroxylase subunits, respectively, and 20% of *tmoC* gene (1936 bp) in pBS(Kan)T4MO were amplified using error-prone PCR (epPCR) (Leung et al., 1989). A 100 μL reaction contained 10 m*M* Tris-HCl (pH 8.3), 50 m*M* KCl, 0.001% gelatin, 6 m*M* $MgCl_2$, 0.35 m*M* $MnCl_2$, 1*M* Betaine, 80 ng of template DNA pBS(Kan)T4MO, 0.2 m*M* dATP and dGTP, 1 m*M* dCTP and dTTP, 5U *Taq* DNA polymerase (Promega, Madison, WI), and 30 pmole of each primer (T4MOEcoRIFront and T4MOABrear, Table I). The T4MOEcoRIFront primer contains an *Eco*RI restriction site located upstream of the *tmoA* gene (Fig. 1), and T4MOABrear is downstream of the naturally occurring *Aat*II site within the *tmoC* gene. A PCR program of 30 cycles of 94°C for 1 min, 52°C for 1 min, and 72°C for 2.5 min, with a final extension of 72°C for 7 min, was used in a Perkin Elmer PCR system 2400 (Perkin Elmer, Norwalk, CT). The resulting randomized PCR product was cloned into pBS(Kan)T4MO after double digestion with *Aat*II and *Eco*RI (New England Biolabs, Beverly, MA), replacing the corresponding fragment in the original plasmid. The resulting plasmid library was transformed into *E. coli* TG1 competent cells via electroporation.

Saturation Mutagenesis

A gene library encoding all possible amino acids at position 100 of T4MO *tmoA* in pBS(Kan)T4MO was constructed by replacing the target codon with NNN via overlap-extension polymerase chain reaction (PCR) (Sakamoto et al., 2001). Two primers, T4MO100Front and T4MO100Rear (Table I) were designed to randomize position 100 of TmoA. Two additional primers for cloning were T4MOEcoRIFront and T4MOBglIIRear (Table I) which encode the *Eco*RI and *Bgl*II restriction enzyme sites; the *Bgl*II site occurs naturally downstream from TmoA position 100 and the *Eco*RI site is upstream of *tmoA* in the multiple cloning site (Fig. 1). *Pfu* DNA polymerase (Stratagene, La Jolla, CA) was used in the PCR to minimize random point mutations, and pBS(Kan)T4MO was used as the template. The first 366 nucleotide degenerate fragment was amplified by PCR using primers T4MOEcoRIFront and T4MO100Rear, and the second degenerate fragment of 663 nucleotides was amplified by PCR using primers T4MO100Front and T4MOBglIIRear. After purifying

Table I. Primers used for mutagenesis (error-prone PCR of TmoA and saturation mutagenesis of TmoA I100) and sequencing of the *tmo* locus in pBS(Kan)T4MO. Restriction enzyme sites indicated in the primer name are underlined.

Primer	Nucleotide sequence
Mutagenesis	
T4MOEcoRIFront	5′-TACGGAATTCAAGCTTTTAAACCCCACAGG-3′
T4MOABRear	5′-TCCATGCTCTTCACTGTTGAC-3′
T4MO100Front	5′-CACTTTGAAATCCCATTACGGCGCCNNNGCAGTTGG-3′
T4MO100Rear	5′-GCTGCATATTCACCAACTGCNNNGGCGCCGTAATGG-3′
T4MOBg1IIRear	5′-TCCAAGCCCAGATCTATCAACGAGCGTTCG-3′
Sequencing	
T4MOEcoRIFront	5′-TACGGAATTCAAGCTTTTAAACCCCACAGG-3′
T4MO-1	5′-CCCGCATGAATACTGTAAGAAGGATCGC-3′
T4MO-2	5′-GCTCGTTGATAGATCTGGGCTTGGACAA-3′
T4MO-3	5′-AATCTATTGAAGAGATGGGCAAAGACGC-3′

from agarose gels, the two fragments were combined at a 1:1 ratio as templates to obtain the full-length degenerate PCR product (981 bp) using T4MOEcoRIFront and T4MOBglIIRear as primers. A PCR program of 30 cycles of 94°C for 1 min, 55°C for 1 min, and 72°C for 2 min, with a final extension of 72°C for 7 min was used. The resulting PCR product containing randomized nucleotides at TmoA position 100 was cloned into pBS(Kan)T4MO after double digestion with *Eco*RI and *Bgl*II, replacing the corresponding fragment in the original plasmid. The resulting plasmid library was transformed into *E. coli* TG1 competent cells via electroporation.

Screening Method

High-activity mutants were screened based on the instability of the T4MO reaction products. At neutral pH, the catechol derivatives formed from NB auto-oxidize to quinones and semiquinones that readily polymerize and form a red or brown color (Meyer et al., 2002). To enable screening of several substrates after transformation, *E. coli* TG1 colonies were transferred using sterile toothpicks to 3–4 agar plates containing LB medium supplemented with 100 μg/mL kanamycin and 1% w/v glucose. Each plate contained 50 transformants, a negative control [*E. coli* TG1/pBS(Kan)] and the wild-type enzyme TG1(T4MO). Following overnight incubation at 37°C, the colonies were transferred to LB plates containing 100 μg/mL kanamycin and 1 m*M* of the desired substrate (the substrate was added to the LB medium from a 500 m*M* stock solution in ethanol) using a nylon membrane (0.45 micron, Fisher Scientific co., Fairlawn, NJ) which lifted the colonies from the glucose plate and then transferred them to the substrate plate with the cells facing away from the agar. The substrate plates were then incubated at room temperature for 18–48 h. A red or brown halo was formed around transformants producing catechol derivatives from the incorporated substrate. The positive red colonies were re-screened using more cell mass to verify the results.

Enzymatic Activity

Experiments were conducted using exponential-phase cultures obtained by diluting overnight cells to an optical density at 600 nm (OD) of 0.1 to 0.2 and growing to an OD of 1.2. The exponentially growing cells were centrifuged at 13,000 *g* for 8 min at 25°C in a Beckman J2-HS centrifuge (Palo Alto, CA). The collected cells were washed once in Tris-nitrite buffer (50 m*M*, pH 7) to remove residual broth and then resuspended in the same buffer. Two mL of concentrated cell suspensions (OD of 2–5) were contacted with substrate concentrations of 25-300 μ*M* (from a 50 m*M* stock solution in ethanol) in 15-mL serum vials sealed with a Teflon-coated septum and aluminum crimp seal. The specific initial reaction rate was constant over this range of cell biomass. The negative controls used in these experiments contained the same monooxygenase without substrates (plus solvent) as well as TG1/pBS(Kan) with substrates (no monooxygenase control). The inverted vials were shaken at room temperature at 300 rpm on an IKA-Vibrax-VXR shaker (Cincinnati, OH) for 2.5–30 min, then one mL of the cell suspension was removed and centrifuged in a 16M Labnet Spectrafuge (Edison, NJ) for 1–2 min. The supernatant was filtered and analyzed by high-pressure liquid chromatography (HPLC).

For toluene oxidation, the cells were prepared in the same way, but phosphate buffer (50 m*M*, pH 7) was used for washing and resuspending the cells. The serum vials containing exponentially grown cells at a final OD of 5–8 were sealed and then 250 μ*M* toluene was added with a syringe, calculated as if all the toluene is in the liquid phase (actual initial liquid concentration was 90 μ*M* based on Henry's law; Dolfing et al., 1993). The reaction was stopped by adding 1 mL of 500 μ*M* hexadecane in ethyl acetate to the vial with a syringe, and the vial was vortexed thoroughly to ensure full extraction of the toluene. The organic phase was separated from the aqueous phase by centrifugation, and 2–3 μL were injected to the gas chromatograph (GC) column. At least two independent experiments were performed to characterize each strain with each substrate described herein.

Analytical Methods

Oxidation of NB and nitrophenols was measured using reverse-phase HPLC. Filtered samples were injected into a Zorbax SB-C8 column (Agilent Technologies, 5 μm, 4.6 × 250 mm) with a Waters Corporation (Milford, MA) 515 solvent delivery system coupled to a photodiode array detector (Waters 996). The gradient elution was performed with H_2O (0.1% formic acid) and acetonitrile (70:30 0 to 8 min, 40:60 15 min, 70:30 20 min) as the mobile phase at a flow rate of 1 mL/min. Compounds were identified by comparison of retention times and UV-visible spectra to those of authentic standards as well as by co-elution with standards. Calibration curves were made at the maximum wavelength of each compound (e.g., 4-NC at 348 nm and *p*-NP at 317 nm).

The identity of 4-nitrocatechol was confirmed by reverse-phase liquid chromatography-mass spectrometry (LC-MS) using a Hewlett-Packard (Palo Alto, CA) 1090 series II liquid chromatograph with a diode array detector coupled to a Micromass Q-TOF2 (Beverly, MA) mass spectrometer. Separation was achieved using a Zorbax SB-C18 column (3 μm, 2.1 × 150 mm) with a mobile phase consisting of H_2O (0.1% formic acid) and acetonitrile and a gradient elution at 0.3 mL/min starting from 100% H_2O (0.1% formic acid) to 0% in 12 min, with a 3 min hold at the final composition. The Q-TOF2 was operated in negative ion electrospray mode with 3.0 kV applied to the inlet capillary and 75V applied to the extraction cone.

Toluene oxidation by TG1(T4MO) variants was measured by GC using a Hewlett-Packard 6890N gas chromatograph equipped with an EC-WAX capillary column (30 m × 0.25 mm, 0.25 μm thickness; Alltech Associates, Inc., Deerfield, IL) and a flame ionization detector. The injector and detector were maintained at 250°C and 275°C, respectively, and a split ratio of 3:1 was used. The He carrier gas flow rate was maintained at 0.8 mL/min. The temperature program was 80°C for 5 min; 80°C to 205°C at a rate of 5°C/min, 205°C to 280°C at 15°C/min, and 280°C for 5 min. Under these conditions, the retention times for toluene, *o*-, *p*-, and *m*-cresols were 4.2, 27.5, 29.2, 29.4 min, respectively. Hexadecane was used as an internal standard. Retention times were determined by comparisons to neat standards as well as by co-elution with standards.

DNA Sequencing

A dideoxy chain termination technique (Sanger et al., 1977) with the ABI™ Prism BigDye Terminator Cycle Sequencing Ready Reaction Kit (Perkin Elmer, Wellesley, MA) and PE Biosystems ABI™ 373 DNA sequencer (Perkin Elmer, Wellesley, MA) was used to determine the nucleotide sequence of TG1(T4MO) mutants. Four primers were generated from the wild-type T4MO sequence [GenBank M65106, Yen et al. (1991); M95045, Yen and Karl (1992)] for sequencing a total of 2 kb including the *tmoAB* genes and 20% of *tmoC* gene: T4MOEcoRIFront, T4MO-1, T4MO-2, and T4MO-3 (Table I). For determining the sequence of the saturation mutagenesis mutants, only the T4MOEcoRIFront primer was used. Sequence data generated were analyzed using the Vector NTI software (InfoxMax, Inc., Bethesda, MD).

Homology Structure Modeling of TmoA

Residues TmoA 44-240 of the wild-type T4MO α-subunit were modeled into the known three-dimensional structure of soluble methane monooxygenase (sMMO) hydroxylase from *Methylococcus capsulatus* (Bath) (Rosenzweig et al., 1997) (PDB accession code 1MTY) using SWISS-MODEL Server (Guex and Peitsch, 1997; Peitsch, 1995; Schwede et al., 2003). The molecular visualization program, Swiss-PdbViewer, was utilized to visualize and manipulate the molecular model, including performing amino acid substitutions isosterically at TmoA I100 based on residue interactions, steric hindrance, and energy minimization.

RESULTS

Random Mutagenesis of T4MO

Error-prone PCR mutagenesis using both manganese and an unbalanced dNTP mixture (Leung et al., 1989) was used to mutate randomly T4MO of *P. mendocina* KR1. Of the complete 4.7 kb gene cluster, 1.9 kb were subjected to mutagenesis, including the entire α and γ fragments of the hydroxylase protein (TmoA and TmoB) and 20% of the ferredoxin protein (TmoC). The mutant library was initially plated on LB Kan medium containing glucose to suppress the expression of the monooxygenase (through catabolic repression of the *lac* promoter), thereby preventing the formation of indigo color, which interfered with the screen. The white colonies were then transferred to substrate containing plates (without glucose) using a nylon membrane. Blue color was eventually formed at this stage as well; however, it was easier to detect the red color indicative of catechols when using glucose plates in the initial step. Five hundred fifty colonies were screened on three substrates: NB, *p*-NP, and toluene. Cells expressing wild-type T4MO showed a yellow halo on NB plates due to formation of *p*-NP, and showed no halo on *p*-NP and toluene-containing plates. The negative control TG1/pBS (Kan) was always colorless on all types of plates. Possible catechol-producing mutants showing a red halo were checked again with this assay to verify the results. Two promising mutants forming red color on NB plates, designated NB1 and E4, were sequenced. Both of these mutants were colorless or light blue on LB medium containing kanamycin, as opposed to the dark blue colonies of TG1(T4MO). No TG1(T4MO) variants with increased activity were found for *p*-NP or toluene. An error rate of 0.4–0.5% was obtained in this mutagenesis (9 or 10 bp changes in 1900 bp subjected to mutagenesis), and this error rate is consistent with the literature for similar conditions (Jaeger et al., 2001).

For the epPCR T4MO mutants NB1 (TmoA Y22N, I84Y, S95T, I100S, S400C; TmoB D79N) and E4 (TmoA E64K, I190T, A354G, T377A, G472C), it was not surprising to find most of the mutations in the *tmoA* gene encoding the protein containing the diiron center. Pikus et al. have shown that changes in the region nearest the iron site (Fe_A) can influence the regiospecificity of T4MO (Pikus et al., 1997) and our group has shown similar results with toluene-*o*-xylene monooxygenase (T2MO) of *P. stutzeri* OX1 (Vardar and Wood, 2004) and toluene *ortho*-monooxygenase (TOM) of *B. cepacia*; a change in position 106 of TomA3 of *B. cepacia* (V106A) was found to increase naphthol oxidation by 6-fold and trichloroethylene oxidation by 2.5 fold (Canada et al., 2002). Hence, it was believed that the analogous position in TmoA for mutant NB1, I100, was the most significant for the change in substrate reactivity for NB oxidation, and it was decided to perform saturation mutagenesis at this position and to screen with the same substrates.

Saturation Mutagenesis

Position I100 of *tmoA* was changed to all 20 possible amino acids using saturation mutagenesis, and 300 colonies were screened on NB, *p*-NP, and toluene since it has been reported by Rui et al. (2004) that screening of 292 colonies is sufficient to ensure that all 64 possible outcomes from

the single site random mutagenesis are evaluated with a probability of 0.99. Two mutants showing a red halo on NB plates were sequenced. Both of them displayed dark blue color on LB plates. The new mutants contained the substitutions TmoA I100A and TmoA I100S and their appearance on a NB plate in comparison with TG1(T4MO) and NB1 is presented in Figure 2. Interestingly, I100S had the same amino acid substitution at position I100 as NB1 (found via epPCR mutagenesis and containing six amino acid changes). Additionally, both mutants were isolated three times from the 300 randomly picked colonies (i.e., mutants with several codons leading to the same amino acid changes were isolated).

Toluene Degradation

Mutant E4 showed relatively weak red color on NB plates and therefore was not further characterized. TG1(T4MO) and its mutants NB1, TmoA I100A, and TmoA I100S were evaluated for their ability to degrade toluene, the natural substrate of this enzyme. Toluene transformation was performed using whole cell catalysis with 90 μ*M* of substrate and representative results are presented in Figure 3a. The two single-mutation variants degrade toluene faster than wild-type T4MO by 50–65%, while the epPCR mutant, NB1, is eightfold slower (Table II). The mutants have an altered regiospecificity and produce higher concentrations of *m*-cresol than TG1(T4MO); all three mutants show a similar product distribution (Table II).

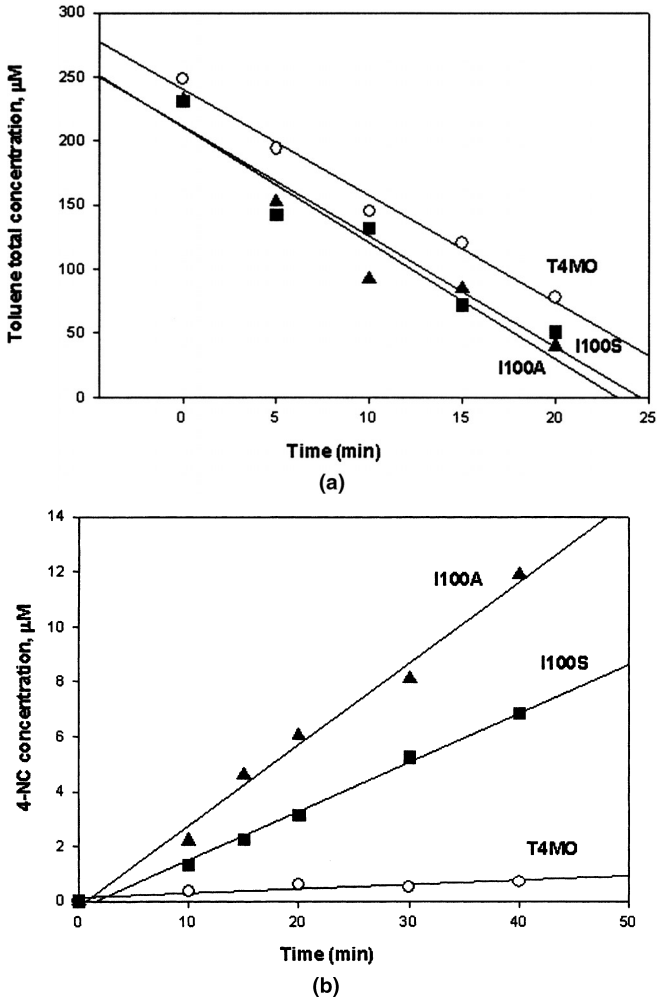

Figure 3. Representative time course experiments for toluene oxidation (a) and 4-NC formation from NB (b) by TG1 cells expressing wild-type T4MO (○), TmoA I100A (▲), and TmoA I100S (■) (regression lines shown). From the slope and biomass of each experiment, the depletion or formation rates in Tables II and III were calculated by averaging values such as these. Total toluene concentration shown includes moles of toluene in both the gas and liquid phases per two mL sample. The initial toluene concentration was 90 μ*M* based on Henry's law constant of 0.27 (Dolfing et al., 1993) (250 μ*M* added if all the toluene in the liquid phase), and the initial NB concentration was 200 μ*M*.

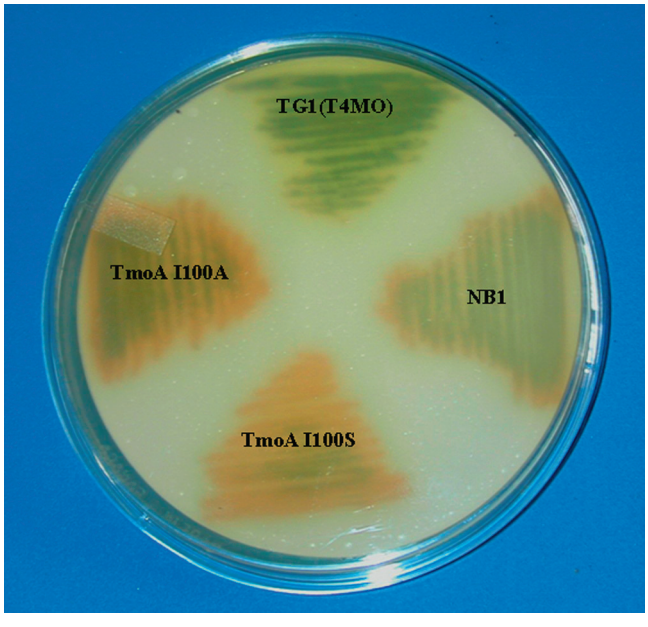

Figure 2. TG1 expressing wild-type T4MO and mutants NB1 (*tmoA*: Y22N, I84Y, S95T, I100S, S400C *tmoB*: D79N), TmoA I100A, and TmoA I100S on LB medium containing 1 m*M* nitrobenzene. The blue portions are cell mass producing indigo, while the orange-red regions are nitrocatechol derivates secreted from the cells following intracellular oxidation of NB.

4-NC Product Distribution From NB and Kinetic Constants

Product formation from NB was measured using reverse-phase HPLC (a representative separation is shown in Fig. 4). For 4-NC formation from TG1 expressing TmoA I100A, the identity of 4-NC was also confirmed by LC-MS by comparison of its mass spectrum with that of an authentic standard [major fragment ions at *m/z* 155 (M, 25) 154 (M-1, 197) 124 (52)]. Whole cell biotransformations were carried out with Tris-nitrite buffer (instead of phosphate buffer) to suppress the reduction of NB to aniline by

Table II. 4-NC formation rates from NB, toluene oxidation rates, and toluene product distribution by TG1 cells expressing wild-type T4MO, TmoA variants, and TOM, and by purified T4MO isoform G103L. Position TomA3 V106 of TOM is analogous to TmoA I100 of T4MO.

Enzyme	4-NC formation from NB,[a] nmol/min·mg protein[b]	Toluene oxidation rate,[c] nmol/min·mg protein[b]	Regiospecificity of toluene oxidation		
			o-cresol, %	*m*-cresol, %	*p*-cresol, %
Wild-type T4MO	0.008 ± 0.001	4.4 ± 0.3	< 1	3	96
NB1 (TmoA Y22N, I84Y, S95T, I100S, S400C; TmoB D79N)	0.0010 ± 0.0002	0.61 ± 0.05	0	20	80
TmoA I100A	0.13 ± 0.01	7.2 ± 1.2	0	20	80
TmoA I100S	0.06 ± 0.011	6.7 ± 1.3	0	21	79
T4moH G103L[d]			55.5	19.7	24.5
Wild-type TOM[e]		1.30 ± 0.06	100	0	0
TomA3 V106A[e]		2.8 ± 0.5	50	33	17
TomA3 V106F[e]		2.1 ± 0.3	28	18	54

[a]Based on HPLC analysis over a 40-min time period. The initial NB concentration was 200 μ*M*. Standard deviations shown ($2 \leq n \leq 4$).
[b]Based on 0.24 mg protein/mL · OD.
[c]Based on GC analysis over a 20-min time period. The initial toluene concentration was 90 μ*M* based on Henry's law constant of 0.27 (Dolfing et al. 1993; 250 μ*M* added if all the toluene in the liquid phase). Standard deviations shown (three or four independent experiments).
[d]Reference Mitchell et al. (2002).
[e]Reference Rui et al. (2004).

the host cells, aerobically grown *E. coli* TG1; in this way, NB was only oxidized by the plasmid-encoding monooxygenases and rates were measured accurately. This change in buffer did not influence the activity of T4MO but reduced the transformation of NB to aniline by TG1/pBS(Kan) to negligible amounts.

To evaluate the product distribution from NB oxidation and to discern the pathway by which 4-NC is produced, whole-cell transformations were performed with 200 μ*M* NB. Following 15 min of incubation, the reaction was stopped by harvesting the cells and the reaction medium was analyzed and quantified using HPLC (Figs. 4 and 5). T4MO is a very regiospecific monooxygenase producing primarily *p*-hydroxylated products (Mitchell et al., 2002; Pikus et al., 1997), and our results with TG1 cells expressing T4MO confirm these findings; however, the three mutants (NB1, I100A, I100S) exhibited lower regiospecificity and produced larger fractions of *m*-NP and 4-NC (Fig. 5). I100A and I100S produced nearly equal amounts of *p*-NP and *m*-NP indicating a drastic change in regiospecificity, much more pronounced than the changes observed for toluene product distribution. The formation rates of 4-NC from 200 μ*M* NB by TG1 expressing wild-type T4MO and the mutants were derived from linear time

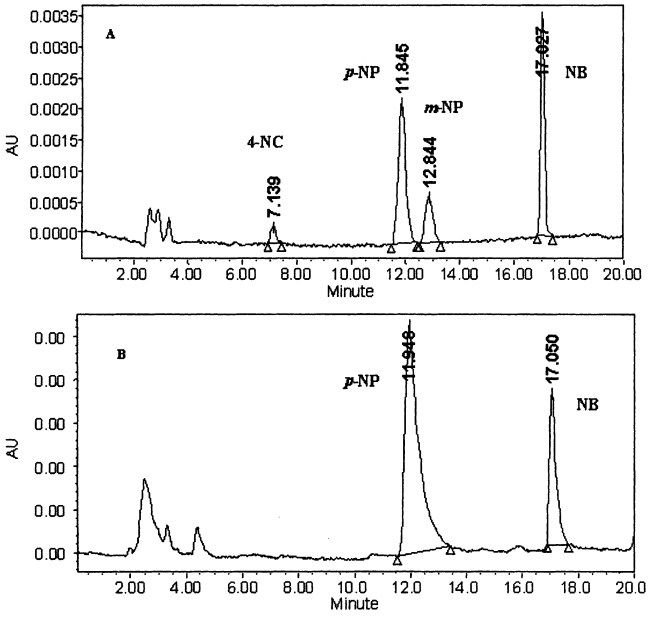

Figure 4. HPLC chromatograms (presented at a wavelength of 348 nm) of NB oxidation by TG1 cells expressing TmoA I100A (A) and wild-type T4MO (B). Initial NB concentration was 200 μ*M* and the contact period was 15 min. The calibration curves and analysis of each compound were obtained at the maximum wavelength for that compound.

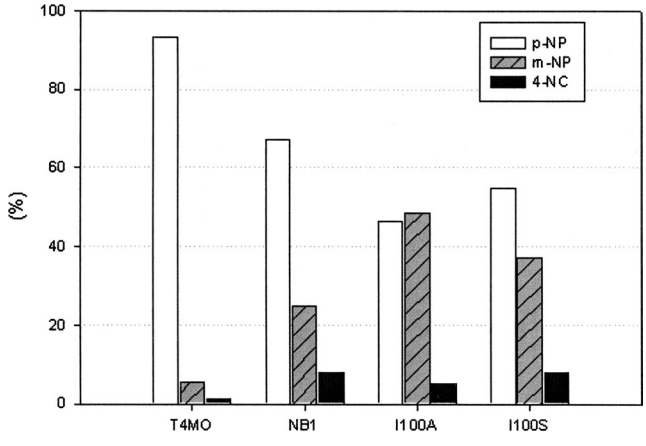

Figure 5. Product distribution observed during oxidation of NB by TG1 cells expressing wild-type T4MO and mutants I100A, I100S, and NB1 (TmoA Y22N, I84Y, S95T, I100S, S400C; TmoB D79N). Initial NB concentration was 200 μ*M*, and the contact period was 15 min. Results represent an average of two independent experiments.

Table III. Apparent V_{max} (nmol/min · mg protein) and K_m (μM) values for T4MO and its TmoA variants towards NB and nitrophenols.[a,b]

Enzyme	NB → *p*-NP			NB → *m*-NP			*p*-NP → 4-NC			*m*-NP → 4-NC		
	V_{max}	K_m	V_{max}/K_m	V_{max}	K_m	V_{max}/K_m	V_{max}	K_m	V_{max}/K_m	V_{max}	K_m	V_{max}/K_m
Wild-type	1.84 ± 0.29	10.9 ± 2.04	0.168	0.16 ± 0.071	89.8 ± 16.7	0.0017	0.16 ± 0.02	50.2 ± 17.1	0.003	0.58 ± 0.033	72.5 ± 5.4	0.008
I100A	0.55 ± 0.012	19.0 ± 2.1	0.029	0.61 ± 0.037	20.3 ± 10.2	0.030	1.5 ± 0.23	115.8 ± 20.5	0.013	3.93 ± 0.26	51.9 ± 3.9	0.076
I100S	0.73 ± 0.07	34.0 ± 7.8	0.021	0.50 ± 0.07	26.3 ± 9.9	0.019	1.09 ± 0.17	38.5 ± 8.4	0.028	2.55 ± 0.014	88.8 ± 3.7	0.029

[a]Initial specific rates were determined for each reaction by monitoring the formation of the product using HPLC; substrate concentrations were 25, 50, 75, 100, 150, 200 μM, and the cell OD was 2 for NB and *m*-NP as substrates, and 4 for *p*-NP as a substrate. Standard deviations shown for two to three independent experiments.

[b]Kinetic constants were calculated from the double reciprocal Lineweaver-Burk plot such as the one presented in Figure 6.

course experiments (Fig. 3b) and are shown in Table II. 3-NC was not observed when NB was the substrate. TG1/pBS(Kan) cells did not oxidize NB, indicating that the NB oxidation was due to the expression of T4MO.

The kinetic constants (apparent V_{max} and K_m) for formation of the nitrophenols from NB, as well as the formation of 4-NC from the intermediate nitrophenols, were measured using whole cells (Table III, representative plot Fig. 6). NB1 (the mutant containing six amino acid changes) had decreased activity for all of the reactions investigated (at a substrate concentration of 200 μM) and therefore its kinetic constants were not measured. TG1 cells expressing the mutant enzymes followed saturation kinetics with all substrates tested (as did wild-type T4MO), and no inhibition was seen by NB or the nitrophenols at concentrations of 200–400 μM (slight inhibition was seen for concentrations greater than 500 μM). Both I100A and I100S showed lower V_{max} values for the transformation of NB to *p*-NP and similar K_m values with wild-type resulting in a six–eightfold decrease in the V_{max}/K_m ratio. In contrast, both mutants had increased V_{max} as well as decreased K_m values in the NB transformation to *m*-NP, resulting in V_{max}/K_m ratios of 11–17 times higher (Table III). It is also evident from the data that the formation of 4-NC from *m*-NP is much faster than from *p*-NP for all the enzymes including wild-type T4MO. Therefore, I100A has 16-fold greater 4-NC production compared to the wild-type T4MO (at saturating substrate levels of 200 μM) since more NB is converted to *m*-NP, which is then rapidly oxidized to 4-NC.

To verify that the increase in activity of mutants I100A and I100S derives from the amino acid substitutions rather than expression level changes, SDS-PAGE was used to visualize two of the six subunits: TmoA (55 kDa) and a combined band from TmoE (35 kDa) and TmoF (36 kDa); mutant and wild-type bands had similar intensities. Fur-

Figure 6. A representative Lineweaver-Burk plot of *m*-NP oxidation to 4-NC by TG1 cells expressing wild-type T4MO (○), TmoA I100A (▲), and TmoA I100S (■) (regression lines shown). Error bars represent the standard deviation from 2–3 independent experiments. The kinetic constants presented in Table III were calculated from such plots.

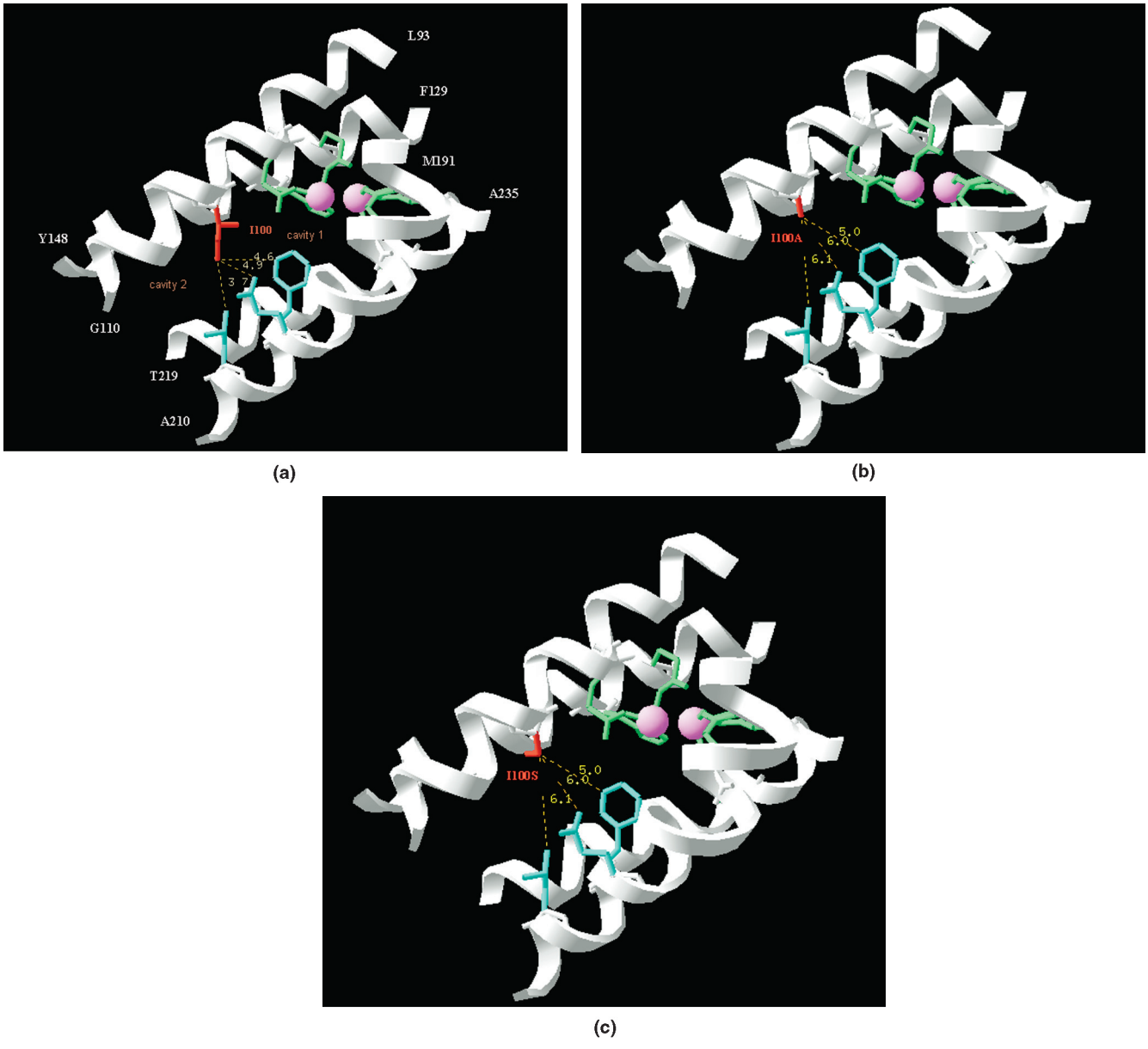

Figure 7. Active site of the TmoA α-subunit showing mutations (in red) at position I100: (a) wild-type I100, (b) I100A, and (c) I100S. Residues in green (E104, E134, H137, E197, E231, and H234) are the coordinate residues anchoring the diiron-binding sites (pink spheres). Portions of the four-helix bundle of TmoA (helix B: P87-F117, helix C: P121-K150, helix E: I186-E214, and helix F: F220-Q243) anchoring the diiron active site are shown in white terminating at L93-G110 (helix B), F129-Y148 (helix C), M191-A210 (helix E), and A235-T219 (helix F). Residues in blue (F205, Q204, and L208) are located spatially opposite I100 and indicate the restricted width of the active site channel (distances from I100 are presented in yellow).

thermore, the ribosome-binding site of the *tmoA* gene in I100A and I100S was unaltered during the mutagenesis as confirmed from DNA sequencing. As the cell growth and the biotransformation conditions were identical for the wild-type and mutants, the changes in activity appear to arise from the mutations at TmoA II100 and not from different expression levels.

TmoA Structural Modeling

To gain insights on the role of I100 in the T4MO active site cavity, a three-dimensional model was constructed (Fig. 7) based on the known crystal structure of hydroxylase MmoX of sMMO (Rosenzweig et al., 1997). Despite the rather low homology between the two enzymes (27% identity), the correct fold was generated as judged by the positions of the diiron coordinating residues in T4MO (E104, E134, H137, E197, E231, and H234) compared to sMMO: the distance between the respective C_α of the iron binding residues was less than 0.1 Å for all six residues. The structural alignment of the template and model also showed conserved spatial configurations.

Although there are limitations to homology modeling, especially in cases of low identity between the enzyme and

the template (Guex and Peitsch, 1997; Schwede et al., 2003), the role of I100 as a part of the hydrophobic cavity around the diiron center is clear. The distances between the Ile side chain and the amino acids in the opposing α helix (F205, Q204, L208) are shown in yellow (Fig. 7a) and highlight the possible function of I100 as a gate restricting the size and conformation of the substrates entering the active site. The size of the channel is increased significantly for mutants I100A (Fig. 7b) and I100S (Fig. 7c) and may provide an explanation for the altered activity and specificity of the mutants.

DISCUSSION

Considering the growing interest in nitrocatechols as important intermediates for drug production (Hartog and Wouters, 1988; Learmonth and Freitas, 2002) and the difficulties in chemically synthesizing substituted nitrocatechols (Palumbo et al., 2002), directed evolution was applied to modify T4MO to increase the level of oxidation activity of NB to 4-NC (a previously undisclosed reaction for T4MO). Successful directed evolution experiments require an effective screening method (Arnold, 1998; Bornscheuer, 2000). In the agar-plate screening method for substituted catechols developed by Meyer et al. (2002), the original protocol called for direct application of *E. coli* transformants onto substrate plates but this was modified here to accommodate the nitro-containing substrates since TG1/pBS(Kan)T4MO did not grow well on LB kanamycin plates containing 1 m*M* NB, and other substrates such as *p*-NP inhibited growth completely. Therefore, the method was revised to include an initial step of growing the transformants on LB kanamycin plates with 1% glucose. A nitric acid-based buffer was also formulated to reduce undesired reduction of the nitro groups during the kinetic measurements.

From the 550 epPCR colonies screened, two potential mutants were identified and sequenced, but only NB1 showed consistent red color on the NB plates. The regiospecificity of the enzyme was altered (Fig. 5) enabling it to make nearly 5 times as much *m*-NP (24.8% vs. 5.4% by wild-type T4MO), and 6 times the amount of 4-NC (7.8% vs. 1.3%). The mutant was unusual in the number of amino acid substitutions: five coding changes in *tmoA* and 1 change in *tmoB*. In previous work employing random mutagenesis on oxygenases such as toluene dioxygenase of *P. putida*, 2-hydroxybiphenyl 3-monooxygenase of *P. azeliaica* HBP1, and horseradish peroxidase, one or two amino acid substitutions were reported for the first round (Meyer et al., 2002; Morawski et al., 2001; Sakamoto et al., 2001).

The two T4MO variants found via saturation mutagenesis, TmoA I100A and TmoA I100S, produced 4-NC at significantly higher specific rates than wild-type T4MO (16.2- and 7.5-fold respectively) and oxidized the natural substrate toluene at 50–65% greater initial specific activity (Table II). Enhanced activity on the natural substrate has also been found by other groups; for example, Arnold and co-workers (Sakamoto et al., 2001) evolved toluene dioxygenase for accepting 4-picoline and found a mutant with 3.7-fold increased activity towards 4-picoline and 1.5-fold increase towards toluene. Meyer et al. (2002) evolved 2-hydroxybiphenyl 3-monooxygenase for guaiacol oxidation and reported a twofold increase for guaiacol (8.2-fold increase for k'_{cat}/K'_m) and 30% increase for 2-hydroxybiphenyl (the natural substrate) oxidation. Recently, Rui et al. (2004) described various TOM mutants capable of oxidizing naphthalene to 1-naphthol at increased rates of 3- to 10-fold. All of the three characterized mutants in that work oxidized toluene at higher initial specific activities of 60–200% but had lower regiospecificity. It is therefore evident that screening mutants for new reactions can result in variants with increased activity towards the natural substrate albeit at the cost of reduced regiospecificity. Although the mutants obtained here oxidize toluene at a faster rate, they produce significant amounts of *m*-cresol, which would not be productive as toluene is oxidized by *P. mendocina* KR1 to *p*-cresol by T4MO, which is converted to the intermediates *p*-hydroxybenzaldehyde and *p*-hydroxybenzoate that are transformed to protocatechuate (Whited and Gibson, 1991). Hence, the cell favors reduced rates and higher selectivity.

The apparent V_{max} and K_m values for *p*-NP and *m*-NP formation from NB, as well as for 4-NC formation from the nitrophenols explain the pathway by which the mutants operate. TG1 expressing wild-type T4MO produces *p*-NP at a maximum rate of 1.84 ± 0.29 nmol/min·mg protein and *m*-NP at a rate which is 11 times slower. *p*-NP is oxidized very slowly to 4-NC by wild-type T4MO and therefore the overall formation of 4-NC from NB is negligible. TG1 cells expressing saturation mutagenesis variants I100A and I100S form *p*-NP at a lower V_{max} than wild-type T4MO but produce *m*-NP at substantially higher rates. Therefore, nearly equal amounts of the mono-nitrophenols are formed. Moreover, the formation rates of 4-NC from *m*-NP by the mutants are 4–9 times higher in terms of apparent V_{max}/K_m values than that of wild-type thus enabling the rapid overall double hydroxylation of NB to 4-NC. Although the T4MO variants I100A and I100S found in this work have not been optimized for increased production of 4-NC, their higher V_{max}/K_m ratios compared to wild-type T4MO form a good basis for future work.

V_{max} and K_m values for T4MO have been reported for the purified enzyme only using toluene as a substrate. The K_m values obtained in these studies were 4 μ*M* for wild-type T4MO and 6–9 μ*M* for various mutants (Mitchell et al., 2002; Pikus et al., 2000), however these values are not comparable to our system employing whole-cells and NB and nitrophenols as substrates (although for wild-type T4MO, K_m for oxidation of NB has a similar value with that of toluene oxidation). A similar whole-cell system with a related enzyme, xylene monooxygenase of *Pseudomonas putida* mt-2 expressed in *E. coli* JM101(pSPZ3), was used for oxidation of various substrates (Buhler et al., 2002).

Apparent K_m values of 87 ± 17 μ*M* and 202 ± 8 μ*M* were reported for toluene and pseudocumene, respectively, and these values are on the same order of magnitude as the values reported in Table III. Biotransformation of 1 m*M* NB using whole-cells of *Nocardia* S3 resulted in 3-NC formation at an initial specific rate of 7.8 U/g cell dry weight (Kieboom et al., 2001), which corresponds approximately to 16 nmol/min·mg protein. The rate of 3-NC formation from 1 m*M* *m*-NP for this strain (Kieboom et al., 2001) was ≈ 5 nmol/min·mg protein which is similar to the V_{max} reported here for *m*-NP oxidation to 4-NC by the T4MO mutants here (Table III).

Despite the limitations of homology-based modeling, in recent years it has become a common methodology for studying structure–function relationships in proteins (Bulter et al., 2003; Meyer et al., 2002; Nomura et al., 1999). We have used MmoX of sMMO as a template for constructing the 3-D model of hydroxylase TmoA of T4MO. Position I100 of TmoA is part of the hydrophobic cavity surrounding the diiron binding site and divides the entrance to cavity 1 and cavity 2 (Fig. 7a). It was hypothesized that the analogous residue L110 of MmoX functions as a gate, restricting the size of molecules entering and leaving the active site (Rosenzweig et al., 1997). Wood and co-workers (Canada et al., 2002) who studied the function of the analogous position in TmoA3 of TOM of *B. cepacia* (V106) supplied evidence for this role. Their V106A mutant was able to hydroxylate bulky polyaromatics such as phenanthrene at higher rates, indicating that a decrease in the size of the side chain allows larger substrates to enter the active site. Our current results with TmoA mutants I100S and I100A support this hypothesis and explain the higher rates observed for toluene, NB, and nitrophenol oxidation. By reducing the size of the side chain at position 100, the width of the active site tunnel increases from an average of 4.4 Å to 5.8 Å (Fig. 7) and facilitates access by substrates and the removal of products (as evidenced by the higher apparent V_{max}/K_m values).

The larger cavity also explains the decrease in regiospecificity observed for the mutants. Mitchell et al. (2003) recently reported on the mechanism of aromatic hydroxylation by T4MO. Their model suggests that toluene moves through the active site tunnel in an orientation that allows initial contact of carbons C4 and C3 with the diiron, leading to a 3,4-epoxide intermediate and predominantly *p*-cresol as a product. Such an alignment of the substrate requires a well-defined and stringent hydrophobic active site as depicted from Figure 7a. I100A and I100S deviate from this constraint by increasing the size of the pocket as well as decreasing the hydrophobicity. The substrate possibly now aligns in a way that enables carbons C3 and C2 to interact with the diiron resulting in the formation of a 2,3-epoxide leading to *m*-cresol formation. Moreover, the altered active site may tolerate more favorably the electron-withdrawing NB molecule that is predicted to be the most difficult substrate to hydroxylate on the basis of electronic considerations (McMurry, 2004; Mitchell et al., 2002, 2003). The model also indicates that the hydroxyl residue of Ser in variant I100S was able to form an additional hydrogen bond with Q141, possibly resulting in a more energy-favorable active site conformation.

Overall we have shown that the catalytic properties and regiospecificity of T4MO can be improved by random mutagenesis and saturation mutagenesis. The implications of the amino acid changes on the function of the enzyme were described on the basis of kinetic data and 3-D modeling. We are currently using this information to evolve this and related monooxygenases such as T3MO of *R. pickettii* PKO1 and T2MO of *P. stutzeri* OX1 for nitro, methyl, and methoxy-substituted benzenes as well as for the formation of indigoid compounds.

We thank Mr. A. Kind for performing the LC-MS analysis, and acknowledge that Dr. K. A. Canada of the Wood Laboratory constructed plasmid pBS(Kan)T4MO.

References

Arnold FH. 1998. Design by directed evolution. Acc Chem Res 31(3): 125–131.

Bornscheuer UT. 2000. Directed evolution of enzymes. Chimica Oggi/ Chemistry Today 9:65–67.

Buhler B, Witholt B, Hauer B, Schmid A. 2002. Characterization and application of xylene monooxygenase for multistep biocatalysis. Appl Environ Microbiol 68:560–568.

Bulter T, Alcalde M, Sieber V, Meinhold P, Schlachtbauer C, Arnold FH. 2003. Functional expression of a fungal laccase in *Saccharomyces cerevisiae* by directed evolution. Appl Environ Microbiol 69: 987–995.

Burton SG. 2003. Oxidizing enzymes as biocatalysts. Trends Biotech 21: 543–549.

Canada KA, Iwashita S, Shim H, Wood TK. 2002. Directed evolution of toluene *ortho*-monooxygenase for enhanced 1-napthol synthesis and chlorinated ethene degradation. J Bacteriol 184:344–349.

Dolfing J, van den Wijngaard AJ, Janssen DB. 1993. Microbiological aspects of the removal of chlorinated hydrocarbons from air. Biodeg 4:261–282.

Eaton RW, Chapman PJ. 1995. Formation of indigo and related compounds from indolecarboxylic acids by aromatic acid-degrading bacteria: Chromogenic reactions for cloning genes encoding dioxygenases that act on aromatic acids. J Bacteriol 177:6983–6988.

Guex N, Peitsch MC. 1997. SWISS-MODEL and the Swiss-Pdb Viewer: An environment for comparative protein modeling. Electrophoresis 18:2714–2723.

Haigler BE, Spain JC. 1991. Biotransformation of nitrobenzene by bacteria containing toluene degradative pathways. Appl Environ Microbiol 57:3156–3162.

Hartog J, Wouters W. 1988. Flesinoxan hydrochloride. Drugs of the future 1:31–33.

Huisman GW, Gray D. 2002. Towards novel processes for the fine-chemical and pharmaceutical industries. Curr Opin Biotechnol 13: 352–358.

Jaeger KE, Eggert T, Eipper A, Reetz MT. 2001. Directed evolution and the creation of enantioselective biocatalysis. Appl Microbiol Biotechnol 55:519–530.

Jain RK, Dreisbach JH, Spain JC. 1994. Biodegradation of *p*-nitrophenol via 1,2,4-benzenetriol by an *Arthrobacter sp*. Appl Environ Microbiol 60:3030–3032.

Kadiyala V, Spain JC. 1998. A two-component monooxygenase catalyzes both the hydroxylation of *p*-nitrophenol and the oxidative release of

nitrite from 4-nitrocatechol in *Bacillus sphaericus* JS905. Appl Environ Microbiol 64:2479–2484.

Kieboom J, van den Brink H, Frankena J, de Bont JAM. 2001. Production of 3-nitrocatechol by oxygenase-containing bacteria: optimization of the nitrobenzene biotransformation by *Nocardia* S3. Appl Microbiol Biotechnol 55:290–295.

Leahy JG, Batchelor PJ, Morcomb SM. 2003. Evolution of the soluble diiron monooxygenases. FEMS Microbiol Rev 27:449–479.

Learmonth DA, Freitas AP. 2002. Chemical synthesis and characterization of conjugates of a novel catechol-*o*-methyltransferase inhibitor. Bioconjugate Chem 13:1112–1118.

Learmonth DA, Vieira-Coelho MA, Benes J, Alves PC, Borges N, Freitas AP, Soares-da-Silva P. 2002. Synthesis of 1-(3,4-dihydroxy-5-nitrophenyl)-2-phenyl-ethanone and derivatives as potent and long acting peripheral inhibitors of catechol-*o*-methyltransferase. J Med Chem 45:685–695.

Leung DW, Chen E, Goeddel DV. 1989. A method for random mutagenesis of a defined DNA segment using a modified polymerase chain reaction. Technique: J Methods Cell Molec Biol 1:11–15.

Li Z, van Beilen JB, Duetz WA, Schmid A, de Raadt A, Grieng H, Witholt B. 2002. Oxidative biotransformations using oxygenases. Curr Opin Chem Biol 6:136–144.

McMurry J. 2004. Organic chemistry. Belmont, CA: Thomson Learning Inc. p 528–569.

Meyer A, Schmid A, Held M, Westphal AH, Rothlisberger M, Kohler HE, van Berkel WJH, Witholt B. 2002. Changing the substrate reactivity of 2-hydroxybiphenyl 3-monooxygenase from *Pseudomonas azelaica* HBP1 by directed evolution. J Biol Chem 277:5575–5582.

Mitchell KH, Rogge CE, Gierahn T, Fox BG. 2003. Insight into the mechanism of aromatic hydroxylation by toluene 4-monooxygenase by use of specifically deuterated toluene and *p*-xylene. Proc Natl Acad Sci USA 100:3784–3789.

Mitchell KH, Studts JM, Fox BG. 2002. Combined participation of hydroxylase active site residues and effector protein building in a *para* to *ortho* modulation of toluene-4-monooxygenase regiospecificity. Biochem 41:3176–3188.

Morawski B, Quan S, Arnold FH. 2001. Functional expression and stabilization of horseradish peroxidase by directed evolution in *Saccharomyces cerevisiae*. Biotechnol Bioeng 76:99–107.

Nomura K, Hoshino K, Suzuki N. 1999. The primary and higher order structures of sea urchin ovoperoxidase as determined by cDNA cloning and predicted by homology modeling. Arch Biochem Biophys 367:173–184.

Oppenheim SF, Studts JM, Fox BG, Dordick JS. 2001. Aromatic hydroxylation catalyzed by toluene-4-monooxygenase in organic solvent/aqueous buffer mixtures. Appl Biochem Biotechnol 90:187–197.

Palumbo A, Napolitano A, d'Ischia M. 2002. Nitrocatechols versus nitrocatecholamines as novel competitive inhibitors of neuronal nitric oxide synthase: lack of aminoethyl side chain determines loss of tetrahydrobiopterin-antagonizing properties. Bioorg Med Chem Lett 12:13–16.

Peitsch MC. 1995. Protein modeling by e-mail. Bio/Technology 13: 658–660.

Pikus JD, Mitchell KH, Studts JM, McClay K, Steffan RJ, Fox BG. 2000. Threonine 201 in the diiron enzyme toluene-4-monooxygenase is not required for catalysis. Biochem 39:791–799.

Pikus JD, Studts JM, McClay K, Steffan RJ, Fox BG. 1997. Changes in the regiospecificity of aromatic hydroxylation produced by active site engineering in the diiron enzyme toluene 4-monooxygenase. Biochem 36:9283–9289.

Rosenzweig AC, Brandstetter H, Whittington DA, Nordlund P, Lippard SJ, Frederick CA. 1997. Crystal structures of the methane monooxygenase hydroxylase from *Methylococcus capsulatus* (Bath): Implications for substrate gating and component interactions. Protein Struct Funct Genet 29:141–152.

Rouhi AM. 2003. Fine Chemicals. Chem Engr News 81:37–52.

Rui L, Kwon Y, Fishman A, Reardon KF, Wood TK. 2004. Saturation mutagenesis of toluene *ortho*-monooxygenase of *Burkholderia cepacia* G4 for enhanced 1-naphthol synthesis and chloroform degradation. Appl Environ Microbiol 70:3246–3252.

Sakamoto T, Joern JM, Arisawa A, Arnold FH. 2001. Laboratory evolution of toluene dioxygenase to accept 4-picoline as a substrate. Appl Environ Microbiol 67:3882–3887.

Sambrook J, Fritsch EF, Maniatis T. 1989. Molecular cloning, a laboratory manual. Cold Spring Harbor, NY: Cold Spring Harbor Laboratory Press.

Sanger F, Nicklen S, Coulson AR. 1977. DNA sequencing with chain-terminating inhibitors. Proc Natl Acad Sci 74:5463–5467.

Scharrenburg GJM, Frankena J. 1996. Biokatalyse helpt farmaceutische industrie bij asymmetrische synthese. Chemisck Weekblad 4: 284–286.

Schmid A, Dordick JS, Hauer B, Kiener A, Wubbolts M, Witholt B. 2001. Industrial biocatalysis today and tomorrow. Nature 409:258–268.

Schmid A, Hollmann F, Park JB, Buhler B. 2002. The use of enzymes in the chemical industry in Europe. Curr Opin Biotechnol 13:359–366.

Schwede T, Kopp J, Guex N, Peitsch MC. 2003. SWISS-MODEL: An automated protein homology-modeling server. Nucleic Acids Res 31:3381–3385.

Tao Y, Fishman A, Bentley WE, Wood TK. 2004. Oxidation of benzene to phenol, catechol, and 1,2,3-trihydroxybenzene by toluene 4-monooxygenase of *Pseudomonas mendocina* KR1 and toluene 3-monooxygenase of *Ralstonia picketti* PKO1. Appl Environ Microbiol 70: 3814–3820.

van Beilen JB, Duetz WA, Schmid A, Witholt B. 2003. Practical issues in the application of oxygenases. Trends Biotech 21:170–177.

Vardar G, Wood TK. 2004. Protein engineering of toluene-*o*-xylene monooxygenase from *Pseudomonas stutzeri* OX1 for synthesizing of 4-methylresorcinol, methyhydroquinone, and pyrogallol. Appl Environ Microbiol 70:3253–3262.

Whited GM, Gibson DT. 1991. Separation and partial characterization of the enzymes of the toluene-4-monooxygenase catabolic pathway in *Pseudomonas mendocina* KR1. J Bacteriol 173:3017–3020.

Yen K-M, Karl MR. 1992. Identification of a new gene, *tomF*, in the *Pseudomonas mendocina* KR1. J Bacteriol 174:7253–7261.

Yen K-M, Karl MR, Blatt LM, Simon MJ, Winter RB, Fausset PR, Lu HS, Harcourt AA, Chen KK. 1991. Cloning and characterization of a *Pseudomonas mendocina* KR1 gene cluster encoding toluene-4-monooxygenase. J Bacteriol 173:5315–5327.